Weld Thermal Efficiency of the GTAW Process

A study of the arc energy distribution, material response, and changes in welding parameters using the GTAW process show improved melting and process thermal efficiency as travel speed is increased.

BY R. W. NILES AND C. E. JACKSON

ABSTRACT. The limitations of arc energy input to certain ranges may not provide an adequate means of predicting or controlling mechanical properties when welding hardenable materials. This has been shown in the following investigation to be due, primarily, to the variation in energy distribution which occurs at the welding arc with changes in welding parameters. This energy distribution has been experimentally determined as a function of welding parameters using the GTAW process and has been expressed in terms of thermal energy efficiencies. The total energy entering the base plate and the energy used to melt the weld nugget have been compared with the total arc energy available and expressed respectively as process and melting efficiencies.

Results of this investigation show that the energy distribution at the welding arc can be significantly changed by variations in current level, travel speed, shielding atmosphere, and process selected. An increase in current level and a decrease in the travel speed produces a decrease in the process efficiency when welding with the GTAW process. This indicates that a lower percentage of the available heat enters the base plate material. An increase in travel speed or current level, on the other hand, produces an increase in melting efficiency with the GTAW process indicating that a greater percentage of the available arc energy is used to form the weld bead.

R. W. NILES, formerly a graduate student at the Ohio State University, is now Welding Engineer, Eastman Kodak Company, Rochester, New York. C. E. JACKSON is Professor of Welding Engineering, The Ohio State University, Columbus, Ohio.

Introduction

Of major concern to the welding engineer has been the effect which the heat of welding has on the mechanical properties and structure of materials to be joined. Many methods have been tried in an attempt to predict the effects of the weld thermal cycle on mechanical and structural properties for the various materials and thicknesses encountered. By limiting the energy input to certain ranges, some control of the metallurgically important peak temperatures and cooling rate has been obtained. However, the nonlinear effect of travel speed, current and voltage on the energy input for any process is not generally recognized.

The total energy input developed per unit length in the welding zone may be calculated by the equation:

$$E_t = VA60/S \text{ (joules/linear in.), or} = VA/S \text{ (joules/linear mm)} \quad (1)$$

where:

E_t = Total arc energy input (joules/linear in. or mm)
V = Arc voltage (volts)
A = Arc current (amperes)
S = Arc travel speed (in./min or mm/s)

This approach is limited in its control of metallurgical response because it does not take into consideration changes in the distribution of the arc energy produced by variations in welding parameters.

As shown in Fig. 1, only part of the total arc energy available is transferred to the weldment. Also, only part of the energy which enters the weldment is used to melt the weld bead; the remainder heats up the base metal and forms the heat-affected zone.

An accurate prediction of the quantity of heat or energy (E_1) entering the base metal is needed to predict the metallurgical response. For a given arc energy input, the ratio between the total arc energy and the heat entering the base metal is significant. The particular welding parameters and process selected for use also affect the metallurgical response. In changing from one welding process to another, large variations in metallurgical response can result despite the fact that the total input energy of the two processes is identical. Shultz, Jackson, and others (Refs. 1, 2) have recognized that total energy input may predict only in a general manner the metallurgical response; hence, other methods of control have been suggested. Shultz and Jackson (Ref. 1) show a correlation between weld metal yield strength and bead size or weld nugget area.

Several investigators have studied the relationship of weld metal yield strength to weld metal cooling rates. The cooling rates for weld metal have

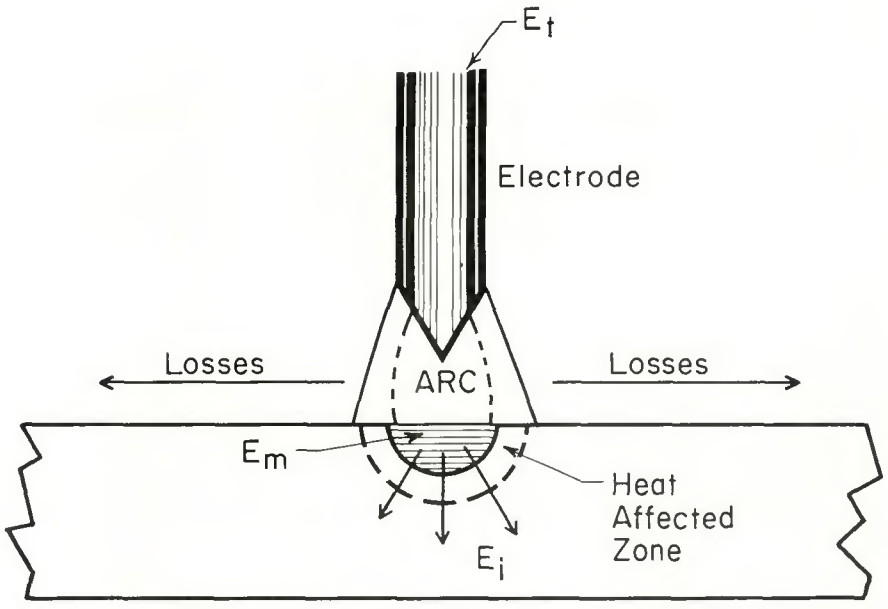

Fig. 1 — Energy distribution at the welding arc. E_t = total energy input/unit length; E_i = total energy entering plate; E_m= energy to melt weld bead; $E_t = E_i$ + losses

been determined experimentally by measuring the weld metal thermal curves with thermocouples inserted into the molten weld pool. Another approach used by many investigators has been to calculate temperature distribution and cooling rates using various mathematical heat transfer expressions (Refs. 3-6). In order to use these and other approaches to predict and control mechanical properties, an understanding of the energy distribution during welding is needed.

Thermal Efficiency

Generally, efficiency is expressed as the ratio of output to input energies. In this investigation, two thermal efficiencies are used to describe the energy distribution in the welding arc. These are referred to as the process efficiency (Z_i) and the melting efficiency (Z_m).

Process Efficiency

The process efficiency (Z_i) is defined as the ratio of the total energy which enters the plate or section being welded per unit distance traveled, to the total energy input of the arc over that same distance. This relationship is stated as follows:

$$Z_i = (E_i/E_t) \times 100 \quad (2)$$

where:

Z_i = Process efficiency (%)
E_i = Energy per unit distance entering the work
E_t = Total arc energy available per unit length

This relationship is important since most heat transfer expressions derived for predicting welding temperature distribution and cooling rates depend upon the insertion of an efficiency term for their solution. If the transfer efficiency of the total energy input is not considered, the energy input term does not represent the actual energy entering the plate.

Melting Efficiency

Equally important is the relationship between melting efficiency and welding parameters. The melting efficiency, Z_m, can be defined as being the ratio of the energy required to melt the weld bead to the total energy input over the same distance. This relationship can be expressed as:

$$Z_m = (E_m/E_t) \times 100 \quad (3)$$

where:

Z_m = Melting efficiency (%)
E_m = Energy per unit length required to melt the weld bead
E_t = Total arc energy available per unit length

The Equation of Heat Distribution

Extensive studies have been carried out by Rosenthal (Refs. 4, 7), Rykalin (Ref. 5), Christensen (Ref. 8) and others. Rosenthal mathematically described the weld thermal cycle for several of the most common welding cases. His work is based on the heat conduction equation as derived by Fourier. Rosenthal assumed in the solution of this equation that:

1. Material physical coefficients were constant.
2. The welding heat source was a point heat source.
3. Heat losses to the surrounding atmosphere were negligible.

Joule heating effects in the plate material were neglected. Ronsenthal has shown that for the case of welding on the surface of a semi-infinite body, the temperature distribution can be expressed by the relationship:

$$T-T_o = (P_{eff}/2\pi kr) \cdot e \exp.(-v/2a)(x + r) \quad (4)$$

where:

T = Temperature of the point in question
T_o = Initial temperature of the point in question
P_{eff} = Effective power input
r = $(x^2 + y^2 + z^2)^{1/2}$ distance from the point in question to the heat source where x, y, and z are the coordinates of position (see Fig. 2).
k = Thermal conductivity (Ref. 9) of the base material which is assumed to be a constant equal to 0.11 cal/(s) (cm^2) (deg C/m).
a = Thermal diffusivity (Ref. 9) of the base material which is also assumed to be a constant equal to 0.12 cm^2/s.
v = Rate of travel of the heat source.

By arbitrarily making the initial temperature level the zero level of temperature, the T_o term may be eliminated and T becomes a measure of the temperature increase at the point in question.

It is important to recognize the limitations of this expression. For example, as "r" approaches zero, the temperature "T" increases to infinity, which is an impossible situation. This results from assuming an infinitely small point heat source when deriving the equation. Since the weld bead which acts as the heat source in the semi-infinite body, is of finite size, the equation is only valid at a distance removed from the fusion area.

Calculation of Process Efficiency, Z_i

In the equation for process efficiency Z_i (eq. 2) E_t can be determined by using eq. 1. E_i can be determined by using Rosenthal's equation for the heat distribution in a semi-infinite body in conjunction with a measured weld thermal cycle. Equation 4 can be expressed in the form:

$$\frac{T - T_o}{P_{eff}} = \frac{e \exp.(-v/2a)(x + r)}{2\pi kr} \quad (5)$$

where all terms have been defined, $T-T_o$ for a particular point in the measured weld thermal cycle can be determined empirically, and since the ratio of temperature to effective

power input is known from application of Rosenthal's equation, the effective power input needed to produce the measured thermocycle can be determined. The effective power input can be converted to joules per unit length for calculation of the process efficiency. Hence,

$$E_i(\text{J/ in.}) = P_{eff}\ (\text{J/ s})\ (60\text{min/ in.}) \quad (6)$$

or

$$E_i(\text{J/ mm}) = P_{eff}\ (\text{J/ s})\ (\text{s/ mm}) \quad (7)$$

and Z can be determined by using eqs. 1 and 6.

Calculation of Melting Efficiency, Z

The weld metal volume represents the total amount of metal which has reached the molten state. This volume has a heat content per unit length proportional to its cross-sectional area which remains constant along the length of the weld bead when constant welding conditions are maintained (Refs. 10, 11). Based on measurements of the nugget area, the calorific heat content of the molten weld bead per unit length can be calculated, compared with the total arc energy available, and used to determine the thermal efficiency of melting.

This is done by calculating first the heat content of a gram of iron heated to the average effective maximum temperature of the weld metal. The maximum temperature of weld metal has been the subject of many investigations. The effective temperature must be above the melting temperature of the base metal. The temperature at the weld metal-base metal interface is at the melting temperature of the base metal. The maximum temperature is dependent upon the process (Refs. 8, 12, 13) and has been generally reported at temperatures below 2000 C with some investigators suggesting temperatures up to 2300 C. The effective temperature will depend upon the arc environment associated with the particular process. For this investigation the effective temperature to which the molten metal has been heated is taken as 1750 C. The heat content of a unit weight of molten weld metal then can be calculated as follows:

The temperature of the weld metal = 1750 C (2023 K)

The heat necessary to melt 1 gram of steel = q

$$q = \Delta H_{p'} = \Delta H_{1800\ k} + \int_{1800}^{2023} C_p\ dT$$

Known quantities are:

ΔH_{1800} = 17.61 kilocalories/ mole weight (Ref. 14)

$C_p{}_{1800}^{2023}$ = 10.5 calories/ mole weight (Ref. 14)

So: $q = 17.61 + \int_{1800}^{2023} 10.5\ dT$

$q = 17.61 + 2.34 = 19.95$ kcal/ mol. wt.

For Fe, mole weight = 55.85 g and 1 calorie = 4.186 joules

Thus, $q = \dfrac{(19.94\ \text{kcal/mol. wt.})\ (4.186\ \text{J/cal})\ (10^{-3}\ \text{cal/kcal})}{55.85\ \text{g/ mol. wt.}}$ (8)

and finally,

$q = 1495.3$ J/ gram

This is the heat necessary to raise one gram of steel to a temperature of 1750 C.

Knowing the heat content of one gram of iron, the calculation of the melting efficiency of the iron weld bead can be made. E_t would be determined from the previously stated relationship of eq. 1. E_m would be determined from the weight of the weld bead per linear millimeter multiplied by the above derived heat content per gram of iron and converted to units comparable to those for E_t. Thus, the weight of the weld metal/ linear mm = nugget area (mm^2) (1 mm) (density of iron) and the weight of weld metal/ linear mm = na (mm^2) (1 mm) (0.00786 g/ mm^3). The heat content per gram of iron is 1495.3 Joules, therefore:

$$E_m(\text{J/ mm}) = \text{na}(mm^2)\ (1\ \text{mm})\ (0.00786\ \text{g/ mm}^3)\ (1495.3\ \text{J/ g}) \quad (9)$$

Now Z_m can be calculated using equations 1 and 9.

Objective

The objective of this investigation was to examine and to show the effect of changes of welding parameters on the energy distribution during welding. The process efficiency of the gas tungsten-arc welding (GTAW) process was studied. The program was aimed also at measuring the melting efficiency with the GTAW process.

Experimental Procedure

Automatic gas tungsten-arc welding systems were used in this investigation to control the welding variables of current, voltage and travel speed. A standard chromel-alumel thermocouple, made from 28 gage wire, was capacitor discharge welded to the top surface of a one-inch thick steel base plate to measure the weld thermal cycle as the welding arc passed its position. Measurements of thermocouple to weld centerline distance, thermocouple to weld edge distance, and weld width were recorded.

The welding parameters used with the gas tungsten-arc welding process in this investigation are reported in Table I. A 5/32 in. (4 mm) diameter 2% thoriated tungsten electrode with conical tipped vertex angles of 30 to 120 deg was used during this investigation. The effects of varying vertex electrode tip angle, shielding gas composition, and current level on the process and melting efficiencies were examined. All weld samples were cross-sectioned and polished. Photomacrographs were taken of the weld and heat-affected zone from which nugget areas and heat-affected zone areas were determined. Using the nugget areas, and applying eq. 9, the calorific heat content per unit length of molten weld metal was calculated for each sample. This heat energy was then compared with the total heat energy developed per unit length by the welding arc to obtain the melting efficiency.

To determine process efficiency, the peak temperature and position were used in calculating the effective power input. Since Rosenthal's equation was derived for a point source traveling in a straight line, and the molten weld bead interface actually acts as the heat source, the edge of the weld bead was used to represent the Y coordinate distance from the thermocouple to the line heat source

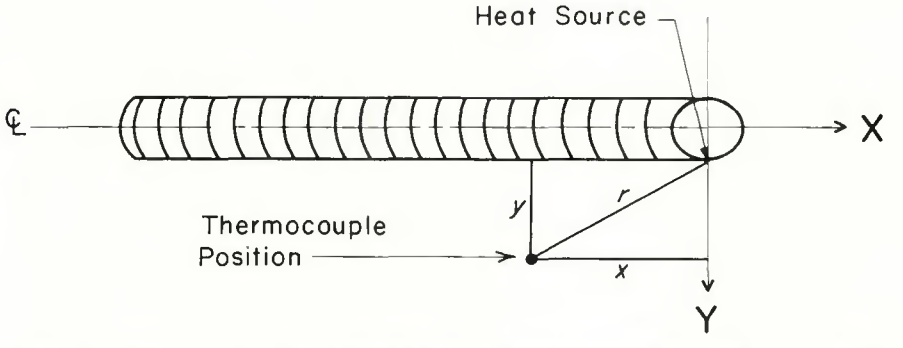

Fig. 2 — Thermocouple position as related to the heat source at the time of the peak temperature

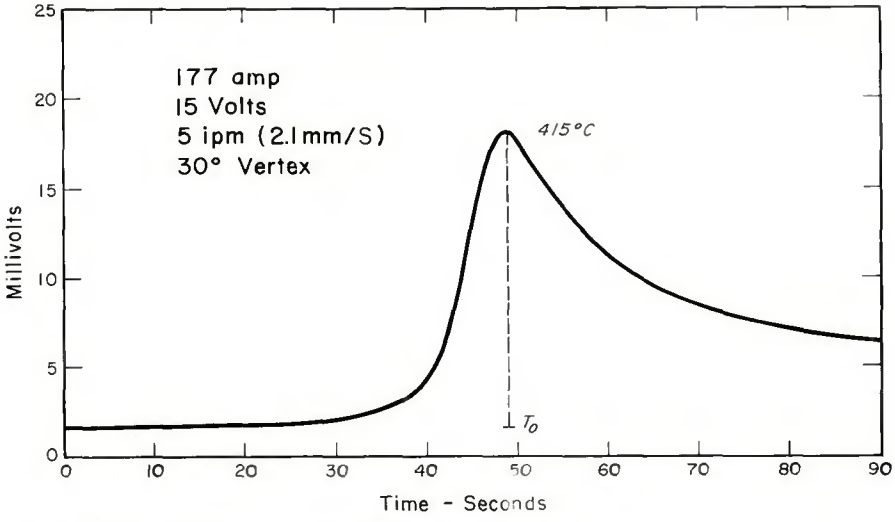

Fig. 3 — Thermal cycle from weld sample number 10.

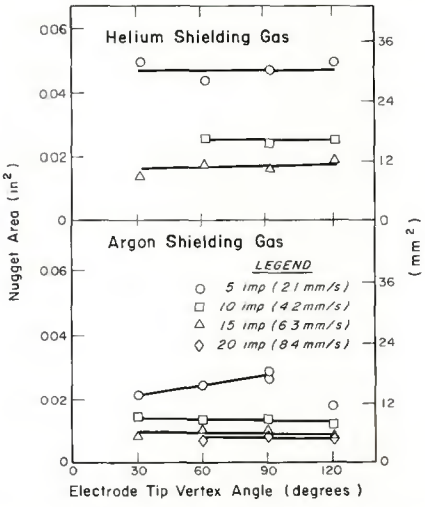

Fig. 6 — Nugget area versus vertex angle for gas tungsten-arc surface welds made on HY-80 plate with an electrode to work distance of 0.10 in. (2.54 mm) and 175 A

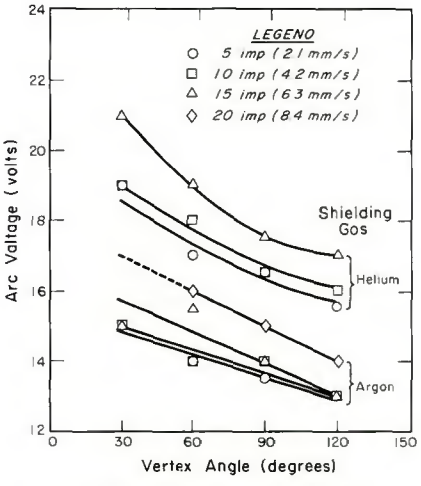

Fig. 4 — Effect of shielding gas and vertex angle on arc voltage for the gas tungsten-arc process with an electrode to work distance of 0.10 in. (2.54 mm) and 175 A on HY-80 plate

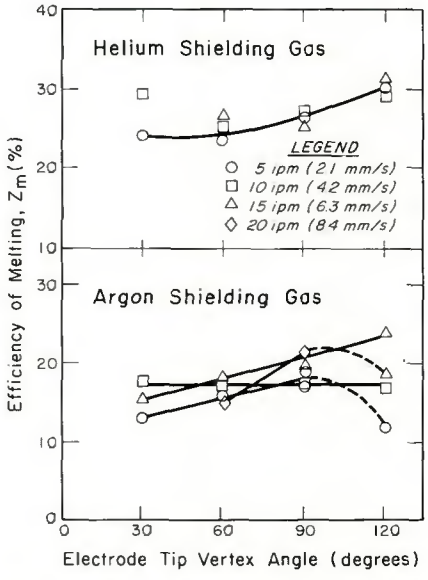

Fig. 5 — Effect of vertex angle on melting efficiency for gas tungsten arc surface welds made on HY-80 plate with an electrode to work distance of 0.10 in. (2.54 mm) and 175 A

as shown in Fig. 2. The distance (r) between the thermocouple and the heat source was used in the calculation of effective power input. Figure 3 shows a typical thermal curve as drawn by a X-Y recorder. The process efficiency was determined by comparing the effective power input with the total arc energy available per unit length.

The bead size or nugget area, heat-affected zone area, process and melting efficiency were determined for each welded sample. These results are reported in Table 1.

Variations in Arc Characteristics Using the GTAW Process

Variations in shielding gas composition and electrode tip vertex angle were investigated for the GTAW welds made on HY-80 plate. An increase in current causes the arc plasma to climb the surface of the conical tip of the electrode. The amount of climb was found to be approximately proportional to the increase in current thus the current density of the emitting surface remained essentially constant. For a small electrode vertex angle, the amount of climb necessary to obtain a certain emitting surface area on the electrode tip was greater than the amount of climb necessary to maintain a given emitting surface area with a larger vertex angle. Since the arc voltage drop is proportional to the length of the arc column, the longer arc column produced with the greater electrode climb for the small vertex angles, produces a greater total arc voltage drop. This was found to be the case in this investigation as illustrated by the results of Fig. 4. Results of similar tests reported by Savage et al (Ref. 15) confirm these observations.

The effect of using argon and helium shielding gases on the arc voltage is also illustrated in Fig. 4. It should likewise be noted that since the arc voltage increases with a decreasing vertex angle while at a constant current of 175 A that the arc energy available also increases with a decreasing vertex angle. As a result, the melting efficiency should increase with increasing vertex angle. This trend was determined for gas tungsten-arc welds made with either helium or argon shielding as shown in Fig. 5. Both of these cases indicate that the heat distribution at the plate surface varies with changes in the vertex angle. As the vertex angle increases, a greater percentage of the heat available in the arc is used to melt the weld nugget. It is also interesting to note that for the two cases where arc instability was observed, due to cathode spot wandering on the 120 deg electrode surface, that the efficiency of melting decreased as shown by the dashed lines of Fig. 5.

As shown in Fig. 6, the weld nugget areas remained essentially constant with changes in vertex angle. The process efficiency results shown in Fig. 7 indicate that the total heat entering the plate material remains essentially constant for changes in vertex angle. Since the melting efficiency, as shown in Fig. 5, increases with increasing vertex angles, this suggests that with increasing vertex angle, an increasing percentage of the total heat entering the plate material is used to form the weld nugget. The ratio of nugget area to heat-affected zone area should therefore increase with increasing vertex

Table 1 — Welding Conditions Used for Gas Tungsten-Arc Weld Beads Made on One Inch Thick Base Plate [a]

Weld no.	Current [b] A	Voltage, V	Travel speed ipm	Vertex angle, deg	Nugget area, $in.^2$	HAZ area, $in.^2$	Total heat transfer efficiency, Z_j (%)	Melting efficiency, Z_m (%)
1	175	14	5	60	0.023	0.043	—	15.13
2	175	14	5	60	0.021	0.036	—	13.82
4	177	15	5	30	0.023	0.041	—	13.66
6	175	13.5	5	90	0.020	0.032	—	13.52
7	175	13	5	120	0.015	0.030	—	10.79
8	175	13	5	120	0.015	0.032	—	10.51
9	177	13	5	120	0.017	0.033	40.19	12.14
10	177	15	5	30	0.022	0.045	38.88	13.18
11	177	14	5	60	0.025	0.037	41.40	15.93
12	177	13.5	5	90	0.028	0.033	36.91	19.01
13	177	14	5	90	0.027	0.030	42.70	17.30
14	177	15	10	30	0.014	0.026	43.33	17.53
15	177	14	10	60	0.013	0.026	43.47	17.23
16	177	14	10	90	0.013	0.022	43.90	17.10
17	177	13	10	120	0.012	0.019	44.58	16.74
18	177	15.5	15	60	0.010	0.017	45.37	18.23
19	177	14	15	90	0.010	0.014	52.83	19.82
20	177	15	15	30	0.009	0.018	53.33	15.67
21	179	13	15	120	0.012	0.015	44.75	24.00
22	176	16	20	60	0.07	0.015	43.30	15.55
23	177	15	20	90	0.009	0.013	45.24	21.49
24	177	14	20	120	0.007	0.010	52.14	18.60
25	174	19	15	60	0.018	0.017	53.64	26.61
26	173	21	15	30	0.014	0.029	50.39	15.56
27	176	17	15	120	0.019	0.023	46.34	30.90
28	175	17.5	15	90	0.016	0.022	51.30	25.63
29	174	19	10	30	0.030	0.034	37.15	29.62
30	175	18	10	60	0.025	0.029	36.49	25.77
31	175	16.5	10	90	0.024	0.026	36.91	27.24
32	176	16	10	120	0.026	0.026	40.16	29.13
33	174	19	5	30	0.050	0.056	37.04	24.16
34	175	17	5	60	0.044	0.056	40.00	23.85
35	176	16.5	5	90	0.049	0.046	38.97	26.37
36	177	15	5	120	0.050	0.038	38.29	30.59
37	125	17	5	60	0.023	0.030	50.43	22.15
38	125	17	10	60	0.017	0.018	50.37	25.50
39	125	17.5	15	60	0.011	0.011	49.75	25.61
40	228	19	15	60	0.027	0.031	44.39	29.90
41	227	19	10	60	0.038	0.053	34.09	28.04
42	227	19	5	60	0.064	0.071	30.98	23.75
43	125	13	5	60	0.011	0.021	63.32	10.96
44	126	13	10	60	0.006	0.013	61.45	12.64
45	124	12.5	15	60	0.005	0.010	60.84	14.89
46	150	13	15	60	0.007	0.012	51.90	16.59
47	150	13	10	60	0.008	0.016	58.32	12.68
48	150	13	5	60	0.015	0.024	40.61	11.98
49	202	14	5	60	0.028	0.034	38.72	15.95
50	199	14	10	60	0.018	0.025	42.98	20.51
51	225	14	5	60	0.031	0.049	32.46	15.90
52	226	14	10	60	0.022	0.028	33.85	22.62
53	225	13	5	60	0.024	0.045	—	13.23
54	200	13	5	60	0.018	0.035	—	10.93
55	175	13	5	60	0.013	0.032	—	9.38
56	175	13	10	60	0.006	0.014	—	8.93
57	175	13	3	60	0.016	0.044	—	6.90
58	150	13	5	60	0.009	0.018	—	7.53
59	150	13	10	60	0.006	0.014	—	10.36
60	150	13	15	60	0.004	0.008	—	9.04
61	125	12.5	5	60	0.006	0.014	—	6.72
62	125	13	10	60	0.002	0.005	—	3.85
63	125	12	3	60	0.006	0.017	—	3.72
64	200	13	3	60	0.024	0.039	—	8.85
65	175	13	5	60	0.020	0.047	—	14.39
66	125	13	5	60	0.010	0.030	—	9.73
67	225	14	5	60	0.030	0.070	—	15.64

(a) Welds 1 to 52 on HY80; 53 to 64 mild steel; and 65 to 67 HY 130.
(b) Electrode negative argon shielding used in all cases except welds 25 to 42, inclusive were shielded with helium.

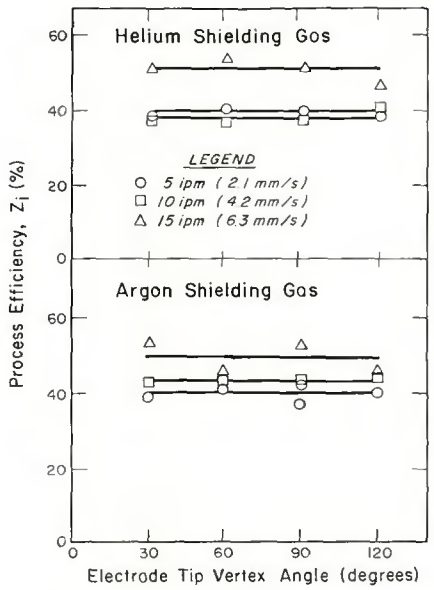

Fig. 7 — Process efficiency versus vertex angle for gas tungsten arc surface welds made on HY-80 plate with electrode to work distance of 0.10 in. (2.54 mm) and 175 A

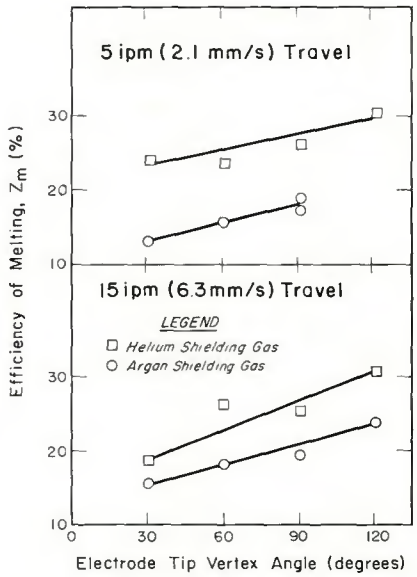

Fig. 9 — Effect of shielding gas and vertex angle on melting efficiency with electrode to work distance of 0.10 in. (2.54 mm) and 175 A

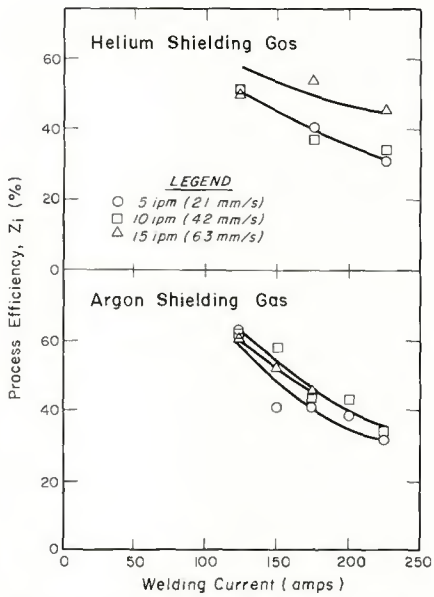

Fig. 10 — Process efficiency versus welding current for gas tungsten-arc surface welds made on HY-80 plate with electrode to work distance of 0.10 in. (2.54 mm)

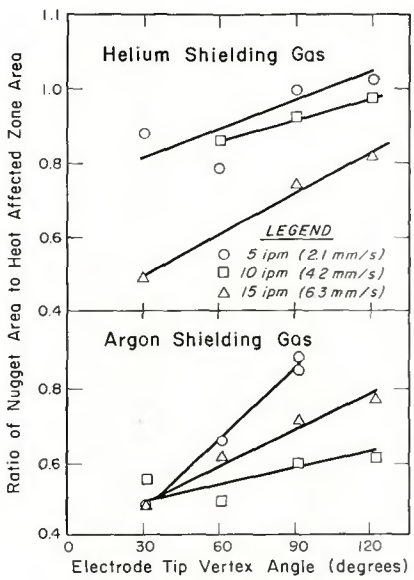

Fig. 8 — Ratio of nugget to HAZ area for gas tungsten arc surface welds made on HY-80 plate using electrode to work distance of 0.10 in. (2.54 mm) and 175 A

angle. This result is shown in Fig. 8 and can be considered significant since the heat-affected zone usually represents the area of greatest change and variation in properties, and any method which could offer an effective means of reducing the size of the heat-affected zone would be of practical importance.

The effect of shielding gas composition on the efficiency of melting for different vertex angle at 5 and 15 ipm (2.12 and 6.35 mm/s) travel speeds is shown in Fig. 9. The greater

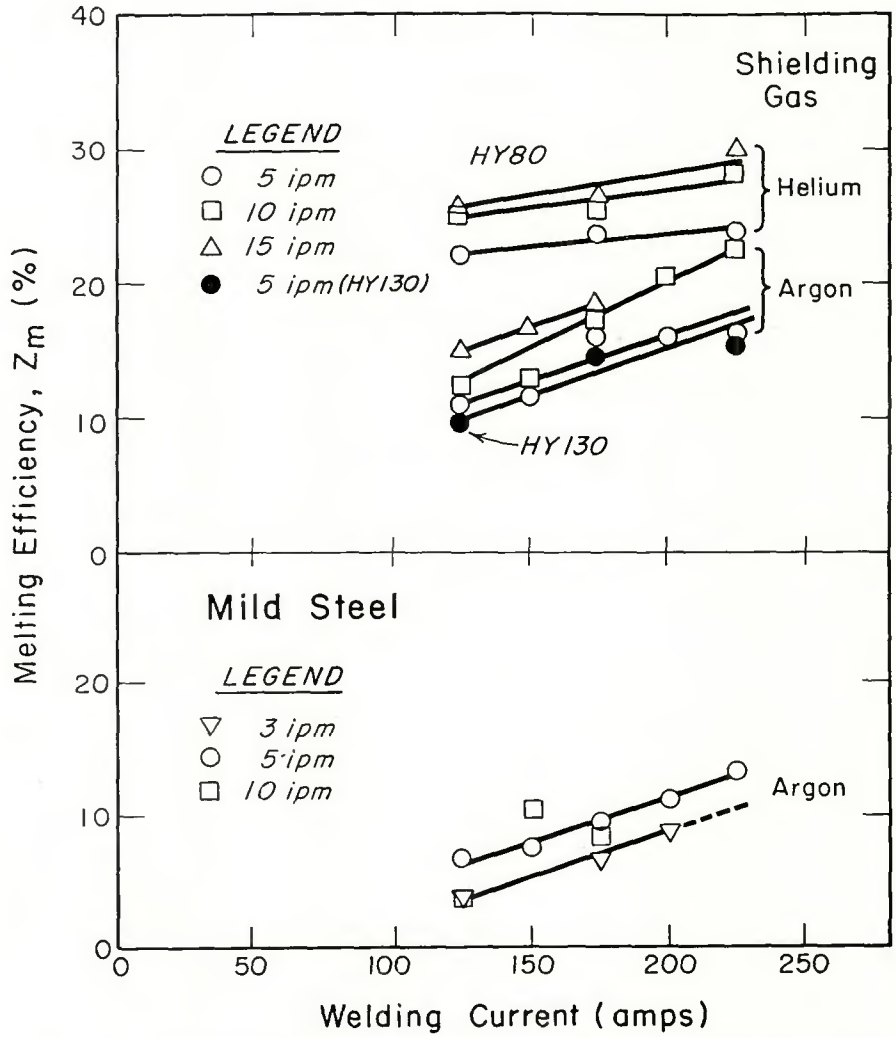

Fig. 11 — Melting efficiency versus welding current for gas tungsten-arc surface welds made on HY-80 plate compared with surface welds made on HY-130 plate and mild steel. Electrode to work distance — 0.10 in. (2.54 mm)

efficiency of melting exhibited by helium at both travel speeds can again be related to the arc characteristics developed. In the arc column, a balance between power input and radial heat losses exists. With the use of helium, a higher heat transfer efficiency gas, the arc column contracts, reducing its surface area in order to balance the heat losses with energy input. This contraction has the effect of increasing the current density of the arc, and since the voltage gradient has also increased, a high power density resulting in higher arc temperature is concentrated on a smaller surface area. The end result of this heat concentration is that a greater percentage of the heat available is used for melting. This results in a higher melting efficiency for helium shielding.

Effect of Welding Parameter Variations on Process Efficiency Using the GTAW Process

A plot of process efficiency versus welding current shown in Fig. 10 indicates that a decreasing percentage of the total heat enters the plate with increasing current levels when using either argon or helium shielding gases. This indicates that heat losses from the arc column increase more rapidly with current level than does the percentage of the total heat entering the base metal. The changes in the process efficiency varying from about 35% to 65% agree favorably with results obtained by Rykalin using calorimetric methods (Ref. 5).

Effect of Welding Parameter Variations on Melting Efficiency Using the GTAW Process

Varying the current between 125 and 225 A and maintaining the vertex angle at 60 deg, the effect of current level on heat distribution was examined. A plot of melting efficiency versus welding current for gas tungsten-arc surface welds made on HY-80 plate, using both helium and argon shielding gas, is shown in Fig. 11. As expected from the previous analysis on the effect of shielding gas compositions, the helium-shielded weld deposits show a higher melting efficiency than those made with argon shielding. Also of significance is the increase in melting efficiency with increasing current and travel speed. The relative increase in the diameter of the arc plasma at the plate surface is small in comparison with the increase in current. Thus, the high heat concentration resulting from the increased current density results in an increased melting efficiency with higher current.

The variations in weld nugget area with current level for the gas tungsten-arc process using helium and argon shielding gases are shown in Fig. 12. As would be expected, the weld nugget area increases with the current level. It is to be noted that the weld nugget areas of the surface beads made with helium shielding are at least twice as large as those made with argon shielding at the same level of current and travel speed.

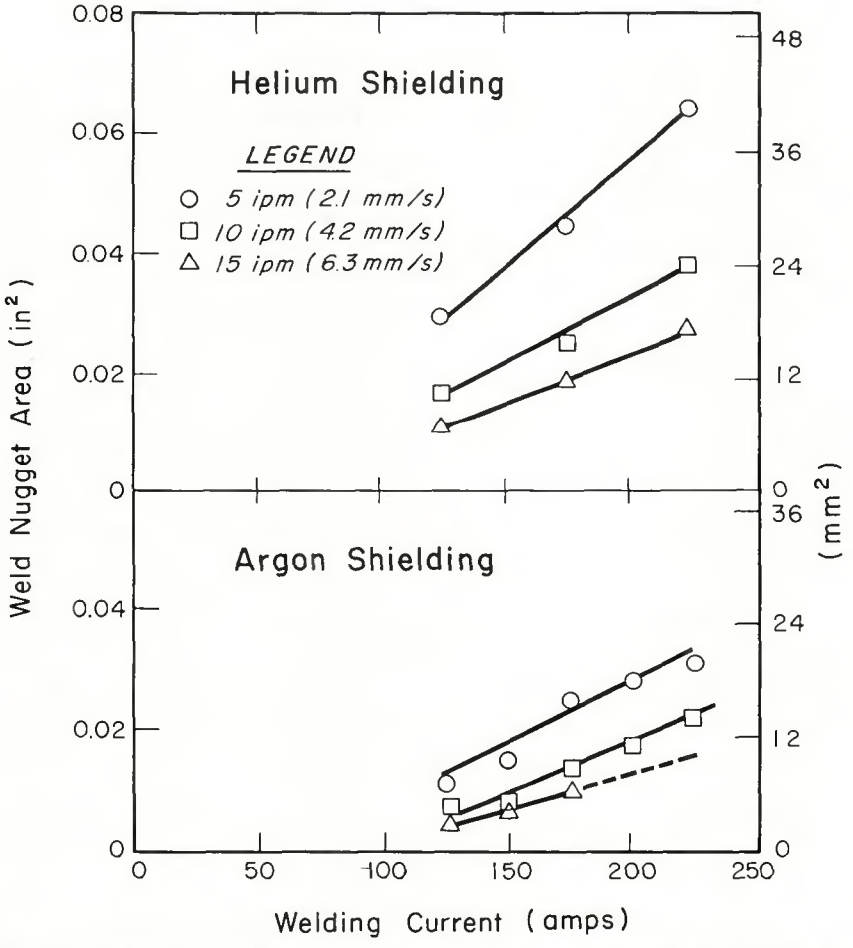

Fig. 12 — Weld nugget area versus welding current for gas tungsten-arc surface welds made on HY-80 steel plate using argon shielding gas. Electrode to work distance of 0.10 in. (2.54 mm)

Conclusions

A description of energy distribution during gas tungsten arc welding has been determined and presented in terms of two weld thermal efficiencies, the process efficiency and the melting efficiency. Through an examination of these efficiencies, better understanding has been gained as to how the welding energy distribution changes as a function of welding parameters and arc variations. Also obtained is an appreciation of how these changes in welding energy distribution may affect the mechanical properties of hardenable materials.

In particular, it has been shown that:

1. The process efficiency remains constant with changes in tungsten electrode tip vertex angle when using the GTAW process, but increased from approximately 40% to 55% with an increase in travel speed from 5 Ipm (2.1 mm/s) to 15 ipm (6.2 mm/s) with either helium or argon shielding. The process efficiency decreases by approximately one-half from 65% to 35% with increasing current level from 125 A to 225 A using the GTAW process and helium shielding. The process efficiency also decreases less drastically with increasing current level at a given travel speed when argon shielding is used with the GTAW process.

2. It is significant in these tests that the ratio of the nugget area to the heat-affected zone area increases as the vertex angle of the tungsten electrode increases.

3. The melting efficiency increases with an increase in the tungsten electrode tip vertex angle when using the GTAW process and increases with a change in shielding from argon to helium gas. The melting efficiency increases with increasing current level and travel speed from approximately 10% to 22% with argon shielding and from approximately 22% to 30% with helium shielding when using the

GTAW process.

The basic relationship and the significance of parameter changes in the GTAW process should be useful as a guide in programming studies for other arc processes. Other processes will undoubtedly show a variation in melting and process efficiencies dependent upon welding arc parameters and material constants.

Acknowledgments

The authors wish to express their appreciation for the support provided by the Union Carbide Corporation, Linde Division. Their financial support provided the Fellowship fund and donations of equipment made the program possible. Technical and material assistance from others is also acknowledged.

References

1. Shultz, B. L. and Jackson, C. E., "Influence of Weld Bead Area on Weld Metal Mechanical Properties," *Welding Journal,* 52 (1), Jan. 1973, Res. Suppl., pp 26-s to 37-s.

2. Jackson, C. E. and Shrubsall, A. E., "Energy Distribution in Electric Welding," *Welding Journal,* 49 (5), May 1950, Res. Suppl,, pp 231-s to 241-s.

3. Adams, C. M., Jr., "Cooling Rates and Peak Temperatures in Fusion Welding," *Welding Journal,* 37 (5), May 1958, Res. Suppl., pp 210-s to 215-s.

4. Rosenthal, D., "Mathematical Theory of Heat Distribution During Welding and Cutting," *Welding Journal,* 20 (5), May 1941, Res. Suppl., pp 220-s to 234-s.

5. Rykalin, N. N., "Calculation of Heat Flow in Welding," translated by Zvi Paley and C. M. Adams, Jr., *Contract Number UC-19-066-001-C3817* 1951, Moscow.

6. Hess, W. F., Merrill, L. L., Nippes, E. F. and Bunk, A. P., "The Measurement of Cooling Rates Associated with Arc Welding and Their Application to the Selection of Optimum Welding Conditions," *Welding Journal,* 22 (9) Sept. 1943, Res. Suppl., pp 377-s to 422-s.

7. Rosenthal, D. and Schmerber, R., "Thermal Study of Arc Welding," *Welding Journal,* 17 (4), April 1938, Res. Suppl., pp 2 to 8.

8. Christensen, N., Davies, L. and Gjermundsen, K., "Distribution of Temperatures in Arc Welding," *British Welding Journal,* Feb. 1965, pp 54 to 75.

9. Carslow, H. S. and Jaeger, J. C., *Conduction of Heat in Solids,* 2nd ed., Oxford University Press, 1959, p 256.

10. Jackson, C. E., "The Science of Arc Welding," *Welding Journal,* Part I, 39 (4), Res. Suppl., pp 129-s to 140-s; Part II, 39 (5), Res. Suppl., pp 177-s to 190-s; Part iil, 39 (6), Res. Suppl., pp 225-s to 230-s, 1960.

11. Jackson, C. E. and Goodwin, W. J., "Effect of Variations in Welding Technique on the Transition Behavior of Welded Specimens, Part II," *Welding Journal,* 27 (5), May 1948, Res. Suppl., pp 253-s to 266-s.

12. Ando, K. and Nishiguchi, K., "Average Temperature of the Molten Pool on TiG and MIG Arc Welding of Steel and Aluminum," *IIW Document 212-161-68,* 1969.

13. Jackson, C. E., "Fluxes and Slags in Welding," *Welding Research Council Bulletin 190,* Dec. 1973.

14. Sims, C. E., *Electric Furnace Steelmaking,* Vol. II, AIME, 1967, p 49.

15. Savage, W. F., Strunck, S. S. and Ishikawa, Y., "The Effect of Electrode Geometry on Gas Tungsten-Arc Welding," *Welding Journal,* 44 (11), Nov. 1965, Res. Suppl., pp 489-s to 496-s.